Cerebral Cortex, 2021;00: 1–15

https://doi.org/10.1093/cercor/bhab360
Original Article

ORIGINAL ARTICLE

Motor Learning Promotes the Coupling between Fast Spindles and Slow Oscillations Locally over the Contralateral Motor Network

Agustín Solano[1], Luis A. Riquelme[1], Daniel Perez-Chada[2] and Valeria Della-Maggiore[1]

[1]IFIBIO Houssay, Department of Physiology, School of Medicine, University of Buenos Aires, C1121ABG, Argentina and [2]Department of Internal Medicine, Pulmonary and Sleep Medicine Service, Austral University Hospital, Buenos Aires B1629AHJ, Argentina

Address correspondence to Valeria Della-Maggiore, IFIBIO Houssay, Department of Physiology, School of Medicine, University of Buenos Aires, 7th Floor, Paraguay 2155, Buenos Aires 1121, Argentina. Email: vdellamaggiore@fmed.uba.ar

Abstract

Recent studies from us and others suggest that traditionally declarative structures mediate some aspects of the encoding and consolidation of procedural memories. This evidence points to the existence of converging physiological pathways across memory systems. Here, we examined whether the coupling between slow oscillations (SO) and spindles, a mechanism well established in the consolidation of declarative memories, is relevant for the stabilization of human motor memories. To this aim, we conducted an electroencephalography study in which we quantified various parameters of these oscillations during a night of sleep that took place immediately after learning a visuomotor adaptation (VMA) task. We found that VMA increased the overall density of fast (≥12 Hz), but not slow (<12 Hz), spindles during nonrapid eye movement sleep, stage 3 (NREM3). This modulation occurred rather locally over the hemisphere contralateral to the trained hand. Although adaptation learning did not affect the density of SOs, it substantially enhanced the number of fast spindles locked to the active phase of SOs. The fact that only coupled spindles predicted overnight memory retention points to the relevance of this association in motor memory consolidation. Our work provides evidence in favor of a common mechanism at the basis of the stabilization of declarative and motor memories.

Key words: human, motor learning, sleep, slow oscillation, spindle

Introduction

In the last decades, the function of sleep in memory consolidation has received extraordinary attention. There is now compelling evidence from human and nonhuman studies (e.g., Plihal and Born 1997; Rasch et al. 2007; Diekelmann and Born 2010; Schönauer et al. 2015) supporting a role of nonrapid eye movement (NREM) sleep in both the stabilization and enhancement of declarative memory (although, see Wamsley 2019; Wang et al. 2021 for recent evidence supporting a similar benefit of post-training rest). The neural signatures of sleep dependent consolidation are rapidly being unraveled. We now know that, during NREM sleep, slow oscillations (SO, ~1 Hz) generated in the cortex (Amzica and Steriade 1998; Timofeev et al. 2000) facilitate the occurrence of thalamic spindles (~10–16 Hz) during their excitable up-state (Steriade 2006; Staresina et al. 2015; Schönauer and Pöhlchen, 2018). A recent study has in fact shown that the induction of thalamic spindles through optogenetics potentiates hippocampus-dependent memories when stimulation is phase-locked with the up-state (active phase) of SOs, whereas spindle suppression impairs memory

formation (Latchoumane et al. 2017). The precise synchrony between fast spindles (≥12 Hz) and SOs, in conjunction with sharp-wave ripples, a hallmark of the *systems consolidation hypothesis*, appears to mediate memory stabilization in a variety of declarative tasks (Buzsáki, 2015; Maingret et al. 2016; Ladenbauer et al. 2017; Helfrich et al. 2018; Muehlroth et al. 2019; Navarro-Lobato and Genzel 2019).

Much less is known about the neural signatures of motor memory consolidation during sleep. Motor learning encompasses motor skill learning (MSL) and motor adaptation. The first involves the acquisition of new motor plans, whereas the second involves the recalibration of pre-existing motor plans (Krakauer et al. 2019). Growing evidence suggests that offline gains observed in humans during motor sequence learning, a type of MSL, are linked to the hippocampus (Albouy, King, et al. 2013; Albouy et al. 2015; Döhring et al. 2017; Schapiro et al. 2019; Jacobacci et al. 2020) and relate to an increment in the density of sleep spindles (Nishida and Walker 2007; Morin et al. 2008; Barakat et al. 2011; Albouy, Fogel, et al. 2013; Boutin et al. 2018). Recent work carried out in rats indicates that learning an MSL task is associated with neural replay over the motor cortex, which is often phase-locked to a SO (Ramanathan et al. 2015) and with an enhancement of the coupling between spindles (fast and slow) and SOs (Silversmith et al. 2020). Nevertheless, whether these changes impact on overnight improvements in performance has not been explored. Finally, a couple of studies framed under the *synaptic homeostasis hypothesis* (SHY), according to which synaptic weights potentiated during wake are downscaled by sleep, have shown that visuomotor adaptation (VMA) increases the power of slow delta waves (~1–4 Hz) during the early portion of NREM sleep (Huber et al. 2004; Landsness et al. 2009). Yet, whether the synchrony between SOs and spindles is relevant for the consolidation of adaptation memories remains unknown.

In this study, we examined if VMA modulates sleep spindles and their coupling with SOs during NREM sleep. Given the role of fast spindles in the consolidation of declarative memories, we also explored the contribution of fast and slow spindles to this process. We have previously shown behavioral evidence supporting the diurnal consolidation of VMA memories within a 6-h window (Lerner et al. 2020). We have also reported that, during this period, the increment in the functional connectivity between motor and parietal areas contralateral to the trained hand predicts overnight memory retention (Della-Maggiore et al. 2017). Here, we addressed whether these local changes in brain activity are further modulated by sleep. To this aim, we took advantage of a protocol focused on the close proximity between learning and sleep, which is known to improve overnight memory retention in declarative and motor tasks (e.g., Schönauer et al. 2015; Sawangjit et al. 2018). After a night of familiarization, volunteers performed a VMA session or a control session, and we quantified the density of spindles (fast and slow) and the coupling between spindles and SOs during NREM sleep. If, as proposed by the systems consolidation hypothesis, the level of coupling between these oscillations is critical for memory stabilization, then the spindle–SO coupling should predict overnight memory retention. Furthermore, to examine the possibility proposed by the SHY, that VMA memories may undergo synaptic downscaling, we also quantified the power of delta waves (~1–4 Hz) early during NREM sleep.

Materials and Methods

Participants

Ten healthy volunteers (five females, age: [mean ± standard error {SE}] 24.3 ± 0.98 years old) complied with the sleep requirements (see below) and completed the whole study. All subjects were right-handed as assessed by the Edinburgh Laterality Questionnaire (Oldfield 1971), and none of them declared neurological or psychiatric disorders. All potential participants were asked to fill the Pittsburgh Sleep Quality Questionnaire (Buysse et al. 1989) and were evaluated on the Epworth Drowsiness Scale (Johns 1991). Only subjects fulfilling the criteria for good sleep quality based on the last two indices were included in the study. Participants were instructed to maintain a regular sleep schedule and to avoid drinking alcohol and coffee during the duration of the experiment. This was monitored through self-recorded spreadsheets provided by the researcher.

All volunteers signed the informed consent approved by the Ethics Committee of the Hospital de Clínicas, University of Buenos Aires (approved on 24 November 2015 and renewed every year), which complies with the Declaration of Helsinki in its latest version and with the National Law on the Protection of Personal Data.

Experimental Paradigm

The VMA task has been described in detail elsewhere (Villalta et al. 2015; Lerner et al. 2020) and will be briefly summarized here. Subjects performed a center-out task consisting of moving a cursor from a start point in the center of a computer screen to one of eight visual targets arranged concentrically 45° from each other using a joystick (Fig. 1A). The latter was controlled with the thumb and index finger of the right hand, while vision of the hand was occluded.

Participants were instructed to make a shooting movement to each target, which were presented one at a time, following a pseudorandomized order (i.e., without following a sequence). As in our previous studies (Villalta et al. 2015; Lerner et al. 2020), cursor feedback was provided continuously from the trial onset throughout the shooting movement (without leaving a trace), and subjects were instructed to make shooting movements through the target, starting as fast as possible from target onset. To avoid online corrections that would lead to submovements, the joystick's gain was set to 1.4 so that a displacement of 1 cm of the tip of the joystick moved the cursor on the screen by 1.4 cm. According to previous pilot data from our lab, this gain yields straight paths with little or no online corrections (reported in Villalta et al. 2015). One cycle consisted of eight trials in which subjects made pointing movements to each of the eight targets, and there were 11 cycles per block.

Subjects performed three different types of trials throughout the study. During perturbed trials a clockwise 45° visual rotation was imposed to the cursor relative to the movement of the hand (see Fig. 1A, right panel). During null trials, that is, unperturbed trials in which no visual rotation was applied, the movement of the cursor directly mapped onto the hand movement. Finally, during error-clamp (EC) trials, visual cursor feedback was manipulated to provide fake "straight" paths to the target, which mimicked those generated during correct trials by projecting the actual movement to the straight line with some additional variability (pointing direction error = 0 ± 10°;

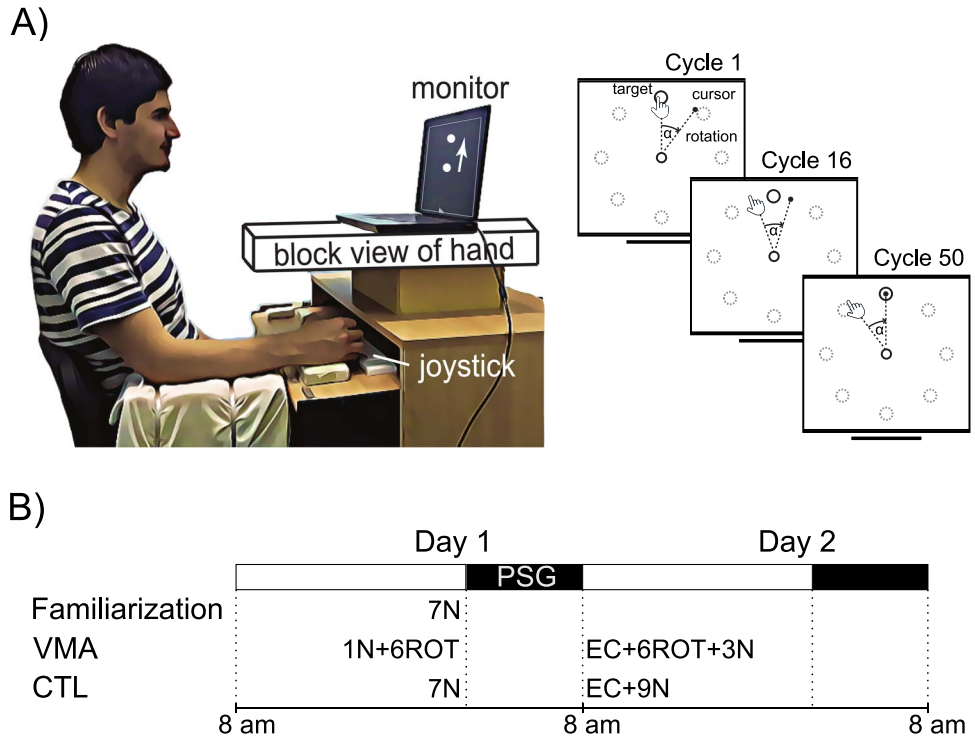

Figure 1. Experimental setup and experimental design. (*A*) *Experimental setup*. Subjects sat on a chair and performed center-out movements to one of eight visual targets using a joystick controlled with their right hand (Left panel). Targets were presented one at a time, following a pseudorandomized order. The right panel is a cartoon representing the visual display; it illustrates the effect of applying the visuomotor rotation (α) over the movement direction of the hand and the cursor as a function of training (cycles). As adaptation progressed over cycles of practice, subjects learned to bring the cursor to the target. (*B*) *Experimental design*. All subjects went through an initial session of familiarization, followed by a VMA session and a control session (CTL), each separated by 1 week. The order of VMA and CTL sessions was counterbalanced. During the familiarization session, they performed seven blocks of null trials (*N*). During the VMA session, they performed one block of null trials followed by six blocks of perturbed trials in which a visual rotation was applied (ROT). On Day 2, retention was assessed using two EC cycles, and then they readapted to the same perturbation (6ROT) and were subsequently washed out (3*N*). During the CTL session, subjects performed the corresponding number of blocks without the visual rotation (*N*). Sleep was monitored overnight with PSG, starting approximately 10 min after performing the task on Day 1.

mean ± standard deviation). EC trials prevent further learning and allow estimating memory retention based on the internal state of the motor system (Criscimagna-Hemminger and Shadmehr 2008; Villalta et al. 2015).

Recent data from our lab using an anterograde interference protocol suggest that consolidation of VMA memories takes place around 6-h postlearning (Lerner et al. 2020). This time window coincides with the period during which VMA memory retention, assessed with EC trials, passively decays exponentially until it reaches an asymptote about 6-h postlearning. Here, we assessed memory retention overnight, 8-h posttraining, as a measure of memory consolidation. The VMA task was implemented in MATLAB (The MathWorks, Inc) using the Psychophysics Toolbox v3 (Brainard 1997; Kleiner et al. 2007).

Experimental Design

We conducted a longitudinal experiment following a within-subjects repeated-measures design, consisting of three sessions that were separated by 7 days each (Fig. 1*B*): 1) a familiarization session during which subjects performed the center-out task during null trials (*N*), that is, in the absence of the visual rotation, 2) a VMA session in which subjects adapted to a visual rotation (ROT), and 3) a control session (CTL) in which subjects performed the center-out task in the absence of the optical rotation (*N*). Thus, the CTL condition served to control for the sensorimotor processing involved in performing the center-out task using a joystick.

We chose a repeated measures design to reduce interindividual variance and to improve statistical power. After the familiarization session, subjects were randomly assigned to the VMA or the CTL condition, each of which took place on a different day and week. The order was counterbalanced so that half of the volunteers performed the VMA condition first and the other half performed it second. The familiarization session was included for two reasons. First, given that subjects have an internal bias for movement direction, adaptation may even take place in the control condition (e.g., Della-Maggiore et al. 2017). The familiarization session thus served as a first approximation to practice with the joystick and to get acquainted with the experimental paradigm in the absence of the optical rotation. Second, Tamaki and collaborators (2016) have shown that subjects do not sleep well during the first night in a new environment. Familiarization with the experimental setup thus aimed at improving the polysomnographic (PSG) recordings.

Participants arrived to the sleep laboratory at 9 pm and electroencephalography (EEG) electrodes were placed over their scalp following the 10-20 montage. Next, they performed the center-out task and went to bed approximately 10 min later for a full night of sleep. A PSG recording was obtained throughout the night. During the familiarization session, participants performed seven blocks of the task without any perturbation

(7*N*). During the VMA and CTL sessions, subjects performed the task before (Day 1) and after (Day 2) a full night of sleep. In the VMA session, on Day 1, they performed one block of null trials (1*N*) followed by six blocks of perturbed trials in which the visuomotor rotation was applied (6ROT). On Day 2, they performed two cycles of EC trials to assess retention, which was followed by six blocks of perturbed trials (6ROT) and three blocks of null trials (3*N*) to washout. The CTL session followed the same experimental protocol but the visual rotation was not applied (7*N* on Day 1, followed by EC + 9*N* on Day 2). In all cases, the level of vigilance before performing the task was assessed using the Stanford Sleepiness Scale (SSS) (Hoddes et al. 1973).

PSG Recordings

Eleven surface EEG electrodes were placed over prefrontal, motor, and parietal areas (FC1, FC2, FC5, FC6, C3, C4, P3, and P4) and over the midline (Fz, Cz, and Pz). Electrodes were mounted following the standard 10-20 arrangement (Modified Combinatorial Nomenclature; Oostenveld and Praamstra 2001). Both mastoids were used as references. In addition to EEG electrodes, two electrodes were placed over the periorbital area of both eyes and two additional electrodes were placed over the chin to measure electrooculography (EOG) and electromyography (EMG), respectively. All signals were acquired at 200 Hz, using the Alice 5 EEG equipment (Philips Respironics, PA, EEUU).

EEG Processing

EEG signal was bandpass-filtered between 0.5 and 30 Hz using a FIR filter ("eegfiltnew" function) from the MATLAB's toolbox EEGLAB (Delorme and Makeig 2004), and then processed with the Artifact Subspace Reconstruction algorithm (Mullen et al. 2015) to remove transient and large-amplitude artifacts ("clean_rawdata" function from EEGLAB; threshold = 30). EOG and EMG signals were also bandpass-filtered in order to facilitate sleep scoring (filter cutoff frequencies: EOG = 0.5–15 Hz; EMG = 20–99 Hz). All PSG recordings were sleep-staged manually according to standard criteria of the American Academy of Sleep Medicine (Iber 2004). Namely, 30-s epochs were classified as either wake (W), NREM (NREM1, NREM2, and NREM3), or rapid eye movement (REM) stage. Stage classification was carried out by two independent scorers. Epochs for which they differed on the classification were defined upon reaching a consensus. After stage classification, sleep architecture was determined based on the following measures, expressed in minutes: total sleep time, sleep latency (latency to NREM1), REM latency, total wake time, wake after sleep onset (WASO), and time in NREM1, NREM2, NREM3, and in REM. Sleep efficiency was also computed as the percentage of total sleep time relative to the time interval between lights-off and lights-on (%). Movement artifacts on the filtered EEG signal were detected by visual inspection and were manually rejected.

SOs (0.5–1.25 Hz) and sleep spindles (10–16 Hz) were automatically identified from the EEG signal corresponding to the stages NREM2 and NREM3 by using previously reported algorithms (see below).

Detection of SOs

The algorithm implemented to detect SOs was based on that reported by Mölle and collaborators (2011) and Antony and Paller (2016). EEG signal was bandpass-filtered between 0.5 and 1.25 Hz. To quantify SOs, we first identified zero crossings of the EEG signal and labeled them as positive-to-negative (PN) or negative-to-positive (NP). Those EEG segments between two NP zero crossings were considered SOs if they lasted between 0.8 and 2 s. Next, we computed the peak-to-peak (P-P) amplitude as the difference between the positive peak and the negative peak; this operation always returned a positive number. Finally, we determined the median of the P-P amplitudes for each channel, each subject, and each session and retained those SOs with a P-P amplitude greater than the median value (Mizrahi-Kliger et al. 2018).

Sleep Spindles Detection

The algorithm implemented to detect sleep spindles was based on that reported by Ferrarelli et al. (2007) and Mölle and collaborators (2011). It was run through each channel for each session. First, EEG signal was bandpass-filtered between 10 and 16 Hz before calculating the instantaneous amplitude (IA) and instantaneous frequency by applying the Hilbert Transform (Tort et al. 2010). The IA was used as a new time series and was smoothed with a 350 ms moving average window. Next, those segments of the IA signal that exceeded an upper magnitude threshold (90th percentile of all IA points) were labeled as potential spindles. The beginning and end of potential spindles were defined as the time points in which the signal dropped below a lower threshold (70th percentile of all IA points). Potential spindles with a duration between 0.5 and 3 s were labeled as true spindles; mean frequency, duration, and maximum P-P amplitude were calculated for each true spindle. Finally, spindles were further classified into two types according to their mean frequency: slow spindles with a frequency <12 Hz and fast spindles with a frequency ≥ 12 Hz (Mölle et al. 2011; Cox et al. 2017).

Coupling between SOs and Spindles

After identifying spindles and SOs, we looked for spindles that occurred during a SO. We quantified spindle–SO couplings according to the following criterion: If a spindle had its maximum P-P amplitude during the course of a SO, it was counted as a spindle–SO coupling.

To characterize further the level of association between these oscillations, we explored the phase of the SO at which the spindle occurred by using the method reported by Tort et al. (2010) and Niknazar et al. (2015). To this end, the instantaneous phase (IP) of each SO was first obtained through the Hilbert transform. The IP of an oscillation varies in a range of $\pm\pi$ radians, so we arbitrarily fixed the SO's positive peak to 0 radian and the negative peak to either $+\pi$ or $-\pi$ radians (PN and NP zero crossings occurred at $+\pi/2$ and $-\pi/2$ radians, respectively). The phase relationship for each spindle–SO coupling was defined as the phase of the SO at which the spindle developed its maximum P-P amplitude. This algorithm was applied to each channel of each session.

Data Analysis

Behavior

Motor performance was measured based on the movement direction of the joystick relative to the line segment connecting the start point and target position (pointing angle). Trials in which the pointing angle exceeded 120° were excluded from further analysis. Given that trials were structured in cycles of eight targets, trial-by-trial data were converted into cycle-by-cycle time series by computing the median pointing angle for

each cycle and each subject. To assess memory retention for each subject, the pointing angle for each EC cycle was expressed as a percentage of the pointing angle asymptote (defined as the median of the last block of learning) and was then averaged.

EEG Signal

SO and spindle measures. As described above, SOs and spindles were automatically identified from the EEG signal that was previously classified as NREM2 and NREM3. Given that some electrodes came off after the first 2 h of EEG recording, we focused the EEG analysis on the first sleep cycle, which was defined as the signal spanned between the onset of NREM1 and the end of the first REM cycle (note, however, that only the EEG signal corresponding to the NREM2 and NREM3 periods were analyzed in this study). The following measures were computed for sleep spindles: duration (ms), mean frequency (Hz), P-P amplitude (μV), and density of fast and slow spindles (number of sleep spindles per minute of NREM2 or NREM3 sleep). Density was also computed for SOs (number of SOs per minute of NREM3 sleep). To characterize the spindle–SO coupling, we computed the proportion of coupled spindles, the density of spindles coupled with a SO (number of spindle–SO couplings per minute of NREM3 sleep), and their coupling phase.

To assess how these measures differed between VMA and CTL, we computed their relative difference according to the function ((VMA − CTL)/CTL*100) for each EEG channel and each subject. We first conducted a global statistical analysis on this measure across the 11 electrodes for each of the sleep metrics of interest. To illustrate the spatial distribution of the effects, we report the results for VMA, CTL, and their relative difference in topographic maps (MNE-Python; Gramfort et al. 2013). Furthermore, to explore the possibility of a local—contralateral—modulation (Nishida and Walker 2007; Johnson et al. 2012; Della-Maggiore et al. 2017; Geva-Sagiv and Nir 2019), we also conducted separate statistical analyses on the data pooled across the channels of the left hemisphere (LH: electrodes FC1, FC5, C3, and P3) and right hemisphere (RH: electrodes FC2, FC6, C4, and P4). Given that the midline may capture electrical activity from both hemispheres, it was excluded from this analysis.

In order to study the level of synchrony between fast spindles and SOs, we determined the phase of the SO at which the spindle yielded its maximum P-P amplitude and contrasted the level of grouping of spindles around the mean phase for the VMA and CTL sessions. Specifically, we first computed the mean coupling phase for each subject and across subjects in polar co-ordinates and displayed them in circular plots. The level of synchrony was then assessed by comparing the variance of the individual coupling phase around the mean across sessions.

To illustrate the synchrony and phase relationship between SOs and spindles, the grand average of the EEG signal filtered in the SO frequency band (0.5–1.25 Hz) and the grand average of the fast sleep spindles frequency band (12–16 Hz) were graphically overlaid, time-locked to the spindle's maximum amplitude.

Delta power. Previous studies (Huber et al. 2004; Landsness et al. 2009; Wilhelm et al. 2014) have shown that training on a VMA reaching paradigm induces a local increase in the power of delta (1–4 Hz) over the anterior and medial portions of the posterior parietal region during the beginning of NREM sleep. The authors have interpreted this finding within the frame of the SHY of slow-wave sleep (Tononi and Cirelli 2003, 2006). According to SHY, the membrane potential of cortical neurons oscillates at a slow frecuency, which can be measured as an increment in the power of the delta band. The delta activity is homeostatically regulated, increasing after wakefulness and returning to baseline during sleep (Tononi and Cirelli 2006). It has been suggested that delta homeostasis may reflect synaptic changes underlying a cellular need for sleep (Tononi and Cirelli 2003). If this was so, local synaptic changes induced during learning should lead to an increment in delta activity that may benefit neural function. Thus, empirically, SHY would manifest as an increment in the power of delta during the beginning of sleep that decreases as the night progresses (Tononi and Cirelli 2006).

To test this hypothesis in our data, we followed the same preprocessing steps (Huber et al. 2004), that is, computed the EEG power density for the first and last 30-min periods of artifact-free NREM sleep and then averaged it for each period within the bandwidth of the delta waves (1–4 Hz). This was carried out for each channel and each session (VMA and CTL). The value corresponding to each channel was then normalized by the average of all channels. As for the other sleep metrics, relative changes in the power of delta activity were computed using the function ((VMA − CTL)/CTL*100).

Statistical Analysis

The sample size of this study ($n = 10$) was determined based on a priori power analysis (simulation approach based on DeBruine and Barr 2021 and Kumle et al. 2021) conducted on the study by Huber and collaborators (2004) in which they examined the impact of VMA on the power of delta oscillation (1–4 Hz) by using the same within-subject experimental design and a similar experimental paradigm.

Parametric statistics were used to analyze all metrics of interest. Analyses were carried out using R (version 3.4.1; R Core Team 2017) in "RStudio" (Rstudio Team 2015). Statistical differences were assessed at the 95% level of confidence (alpha = 0.05), and were carried out by fitting linear mixed models (LMM; using the "lmer" function implemented in the "lme4" package in R; Bates et al. 2015). Random intercepts and random slopes of LMMs were estimated for each subject to take into account the repeated measures across sessions. The response variable was either the relative difference between sessions ((VMA − CTL)/CTL*100) or the measures corresponding to the VMA and CTL conditions. The fixed effects were the condition (VMA or CTL), sleep stage (NREM2 or NREM3), the type of spindle (fast or slow), the hemisphere (LH or RH), the sleep stage by spindle-type interaction, and the hemisphere by sleep stage interaction, depending on each analysis.

Our LMM models included the data from each electrode as replications (the LMM takes into account the dependence between replications through the estimation of random effects; Bates et al. 2015). To assess the statistical significance of fixed effects, we used *F* tests or *t*-tests with Kenward-Roger's approximation of the degrees of freedom to obtain the corresponding *P* values (Halekoh and Højsgaard 2014). Note that in cases where the value of a replication deviates beyond 2.5 median absolute deviation (Leys et al. 2013), the degrees of freedom may not result in an integer.

To analyze the phase relationship between spindles and SOs, the Rayleigh test was used to establish whether the sample distribution of phases was uniform or unimodal for each condition (Pewsey et al. 2013). The null hypothesis is that observations are uniformly distributed. Thus, a significant Rayleigh test is indicative of a preferred phase relationship between spindles and SOs. To compare the preferred mean phase between the VMA and

Table 1 SSS; shown are the mean and SE of SSS scores assessed during the VMA and CTL conditions before doing the motor task; statistical results, using *t*-tests, show that the score in all sessions was ≤ 3, consistent with a mental state of vigilance

		SSS		One sample *t*-test	
		Mean score	SE	*t*	*P*
CTL	Day 1	3.0	0.42	0	0.5
	Day 2	2.2	0.29	−2.75	0.98
VMA	Day 1	2.7	0.42	−0.71	0.75
	Day 2	2.4	0.31	−1.96	0.96

CTL conditions, we used the Watson-Williams Test for von Mises distributions. The null hypothesis is that both conditions share a common mean phase; hence, a significant result indicates that the phase differs across conditions. Finally, to assess whether the level of grouping of the phase differed across conditions, we used the Fisher's test for Von-Mises distributions. This test evaluates the common concentration of the phases around the mean between conditions. The null hypothesis is that samples are equally concentrated. Therefore, a significant test indicates that the concentration of the phases around the mean differs across conditions. All tests were implemented in the "circular" R package (Agostinelli and Lund 2017).

Finally, to examine if the density of SO-coupled and uncoupled spindles predicted overnight memory retention, a Pearson correlation was computed for each measure and was corrected for multiple comparison using the Bonferroni correction (adjusted alpha level = 0.025 to correct for two correlations). We computed accurate confidence intervals (CIs) of the correlation coefficient based on the empirical distribution generated using the Bootstrap approach (Efron and Tibshirani 1993), which has no a priori assumptions about the data distribution. We calculated the percentile bootstrap 95% CIs for the correlation between the relative change in density of spindle–SO couplings and uncoupled fast spindles with overnight memory retention. Pairs of observations from each sample were initially resampled with replacement, and their correlation coefficient (*r*) was obtained. This procedure, which was repeated 1000 times, generated a distribution for the correlation coefficients. To determine the 95% confidence limits, we then sorted the resulting distribution of *r* and took the values falling at the 2.5 and 97.5 percentiles as our confidence limits.

Results

To study the impact of VMA on brain oscillations, we quantified the sleep metrics described above during the period of NREM of the first sleep cycle. We also examined the sleep architecture to assess whether learning affected any sleep stage/s differentially.

Behavioral Results

All volunteers learned to compensate the visual rotation during the VMA session (Fig. 2A) and, on average, retained 56 ± 10.5% (mean ± SE) overnight (Fig. 2B). In the CTL condition, in which no perturbation was applied, pointing angle oscillated around zero (mean ± SE: 0.38° ± 6.04°) during EC trials.

The degree of vigilance assessed using the SSS yielded scores below 3 (Day 1 and Day 2 for CTL and VMA sessions = $P > 0.5$), consistent with a mental state of alertness both before performing the task at night and the day after (see Table 1).

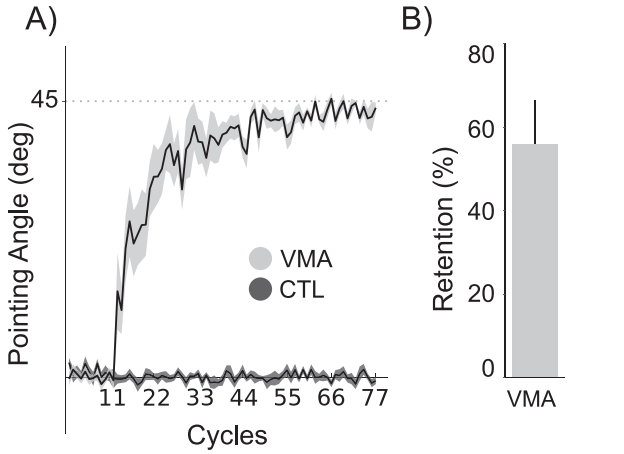

Figure 2. Behavioral performance. (*A*) *Learning curves*. Shown is the mean ± SE of the pointing angle (degrees) for the VMA (light gray shade) and CTL (dark gray shade) conditions during Day 1. All volunteers learned to compensate the visual rotation during the VMA condition. (*B*) *Memory retention*. Memory retention was assessed on Day 2 as the pointing angle for each EC cycle expressed as a percentage of the pointing angle asymptote and was then averaged.

Effect of VMA on Sleep Architecture

We found no significant differences in sleep architecture across sessions for any of the computed measures, suggesting that adaptation did not modulate the intrinsic sleep structure. Their corresponding scores and statistics are displayed in Table 2. The average (mean ± SE) sleep architecture for the first sleep cycle was: NREM1 = 17.4 ± 3.76 min; NREM2 = 30.1 ± 6.73 min; NREM3 = 44.2 ± 4.59 min; REM = 15.9 ± 2.85 min; total sleep = 107.6 ± 12.43 min.

VMA Modulates the Density of Fast Spindles during NREM3

We first looked at the impact of VMA on the intrinsic features of spindles, that is, frequency, duration and P-P amplitude during the first cycle of NREM sleep. No statistical differences were found for frequency (LMM stats, main effect of session: $F(1, 8.73) = 0.04$, $P = 0.84$), duration (LMM stats, main effect of session: $F(1, 8.99) = 0.07$, $P = 0.80$), or amplitude of sleep spindles (LMM stats, main effect of session: $F(1, 8.48) = 0.12$, $P = 0.74$).

Next, we examined the global effect of adaptation learning on spindle density during NREM sleep. Previous work has distinguished between two types of spindles according to their spatial distribution and intrinsic frequency (Mölle et al. 2011; Cox et al. 2017). Fast spindles, which have been linked to memory consolidation (Barakat et al. 2011; Ladenbauer et al. 2017;

Table 2 Sleep architecture

Measure	Familiarization		CTL		VMA		LMM	
	Mean	SE	Mean	SE	Mean	SE	F	P
Total sleep time (min)	376.40	23.97	386.10	8.91	386.85	12.76	0.18	0.83
Sleep efficiency (%)	81.90	5.27	87.36	2.19	86.57	3.11	1.01	0.38
Sleep latency (min)	18.20	4.95	18.40	4.35	16.05	3.40	0.34	0.71
REM latency (min)	132.60	20.81	105.00	9.88	123.85	15.66	1.09	0.35
Total wake time (min)	80.35	24.50	54.80	9.67	58.75	14.48	1.01	0.38
WASO (min)	42.95	19.93	33.10	8.95	29.50	6.40	0.41	0.67
NREM1 (min)	43.35	7.43	53.30	9.69	53.35	5.14	1.17	0.33
NREM2 (min)	157.30	17.68	157.25	11.48	150.15	14.70	0.19	0.82
NREM3 (min)	100.25	12.27	100.15	7.45	105.90	7.43	0.15	0.86
REM (min)	75.50	10.92	75.40	9.23	77.45	8.48	0.03	0.97

Note: Shown are the mean and SE corresponding to the sleep measures listed in the first column for the familiarization, VMA, and CTL conditions. The last column depicts the statistics and P values yielded by comparing the three conditions using LMMs. All measures are depicted in minutes except for sleep efficiency, defined as the percentage of total sleep time relative to the time interval between lights-off and lights-on (%).

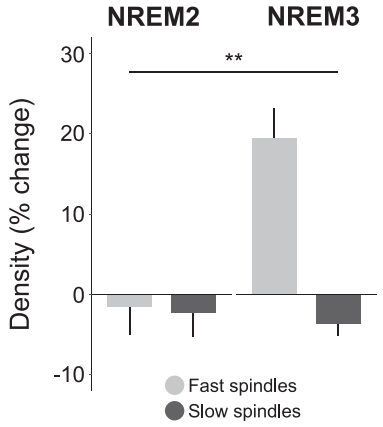

Figure 3. VMA modulates the density of fast spindles during NREM3. The bar plot depicts the relative difference in the density of fast and slow spindles (mean ± SE) between VMA and CTL sessions ((VMA − CTL)/CTL*100) during NREM2 and NREM3. VMA increased the density of fast spindles during NREM3. **$P < 0.01$ indicates the sleep stage by spindle-type interaction.

Helfrich et al. 2018; Muehlroth et al. 2019; Navarro-Lobato and Genzel 2019), are distributed over centro-parietal areas and have a frequency ≥12 Hz, whereas slow spindles are distributed over frontal areas and have a frequency <12 Hz. Here, we explored whether VMA differentially modulated fast and slow spindles. In humans, motor sequence learning has been associated with an increment in the density of fast spindles during NREM2 (e.g., Boutin et al. 2018). Given that we were interested in studying both the number of spindles and their coupling with SOs, which are more prominent during NREM3, we quantified spindle density in both sleep stages.

Figure 3 depicts the effect of VMA on the density of fast and slow spindles during NREM2 and NREM3 (relative change in density, mean ± SE: NREM2: fast spindles = −1.33 ± 3.76%, slow spindles = −3.39 ± 3.28%; NREM3: fast spindles = 22.59 ± 4.21%, slow spindles = −3.42 ± 1.59%). We found a significant stage by spindle-type interaction (LMM stats: $F(3, 14.81) = 8.89$, $P = 0.001$, followed by a one sample *t*-test for fast spindles during NREM3 versus zero: $t(9.68) = 3.57$, $P = 0.005$), suggesting that only the density of fast spindles during NREM3 was modulated by adaptation learning.

Figure 4 illustrates the topographic distribution of fast and slow spindle densities for the VMA and CTL sessions (first two columns) as well as for the relative change between them ((VMA − CTL)/CTL*100). Note that, for both VMA and CTL sessions, fast spindles were observed over parietal and central brain regions, whereas slow spindles were distributed more frontally. Especially salient was the strong modulation of VMA on the density of fast spindles (up to 36%) during NREM3 (third column), characterized by a somewhat asymmetric pattern. Quantification of this effect between LH and RH yielded a significant difference, with the LH showing higher density of fast spindles than the RH (relative change in density, mean ± SE: LH = 30.21 ± 6.35%; RH = 14.97 ± 5.33%; LMM stats: main effect of hemisphere: $F(1, 10.9) = 5.06$, $P = 0.046$). In sum, our findings show that VMA increases the density of fast spindles during NREM3 most preponderantly over the contralateral hemisphere to the trained hand.

Effect of VMA on Slow-Wave Sleep

After studying the activity of sleep spindles, we explored the impact of adaptation learning on slow-wave sleep. Previous work aimed at testing SHY in VMA, using a reaching paradigm (Huber et al. 2004), identified an increment in the power of delta during the first 30 min of NREM sleep that decreased thereafter. The authors interpreted this phenomenon as reflecting an improvement in the signal-to-noise ratio of strongly potentiated—relevant—synapses. To examine the possibility that memories formed with practice in our experimental paradigm may undergo synaptic downscaling during sleep, we followed the analytical approach by Huber and collaborators (see Materials and Methods).

As revealed by Figure 5, VMA increased the power of delta locally, in an interhemispheric manner, during the first 30 min compared with the last 30 min of NREM sleep (LMM stats for hemisphere by segment interaction: $F(1, 120.4) = 4.09$, $P = 0.045$). This finding is consistent with the SHY as a potential mechanism mediating memory stabilization during sleep.

Next, we examined whether VMA modulated the density of SOs (~1 Hz) during the first sleep cycle. Given that SOs are the hallmark of NREM3 and that, as observed in the previous section, sleep spindles were mostly modulated during NREM3, we quantified SOs during this stage (Riedner et al. 2007; Mölle et al. 2011). We found that VMA did not increase the density of SOs above

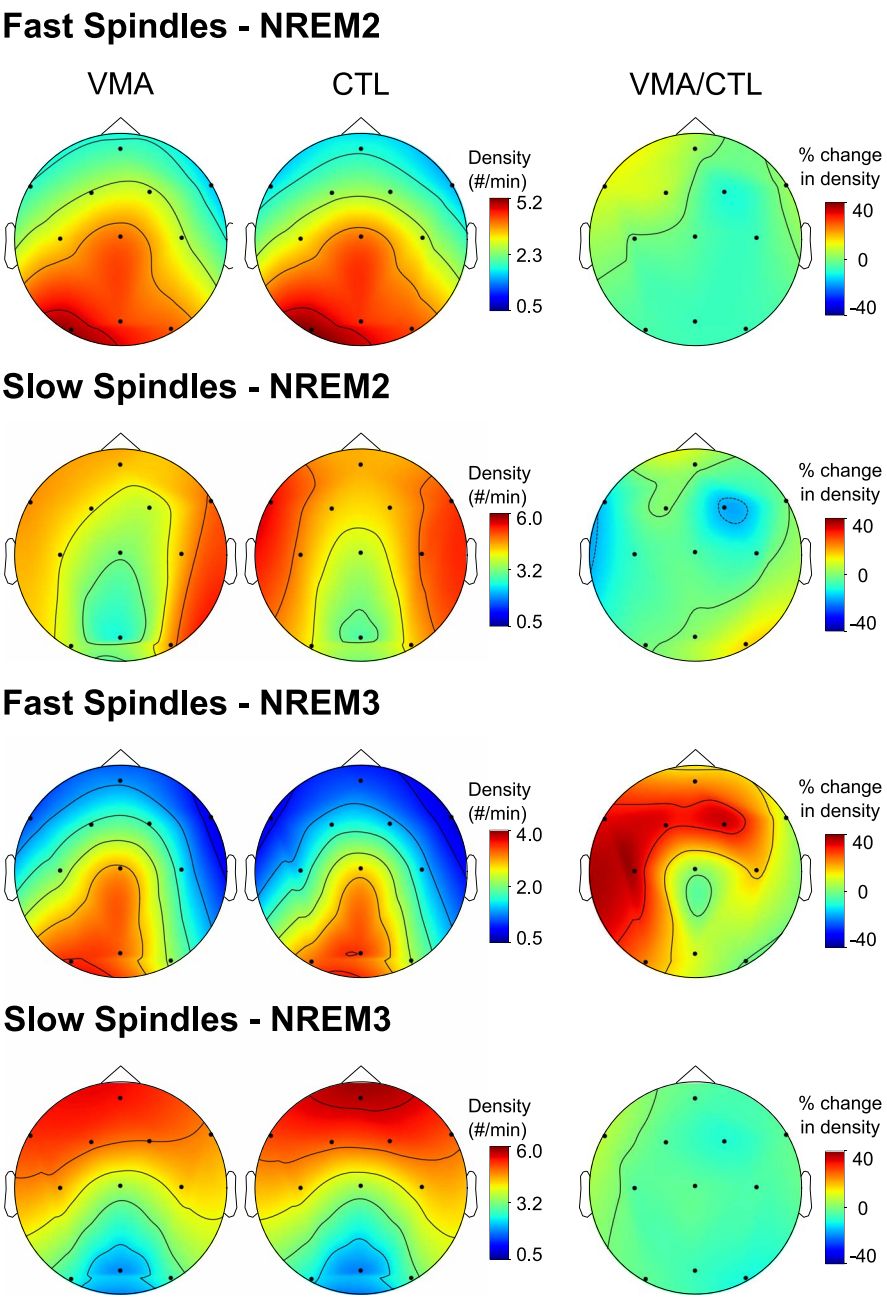

Figure 4. Topographic distribution of the density of fast and slow spindles during NREM2 and NREM3. Shown are the topographic plots for the density of fast and slow sleep spindles (number per minute) corresponding to the VMA session, the CTL session, and their relative difference (VMA/CTL) during NREM2 (upper two rows) and NREM3 (lower two rows). Relative differences between VMA and CTL were computed according to the function ((VMA − CTL)/CTL*100). Color bars represent the density of sleep spindles for the VMA and CTL conditions and their percent change, respectively. Only the density of fast spindles during NREM3 was modulated by adaptation learning (LMM stats: $F(3, 14.81) = 8.89$, $P = 0.001$, followed by a one sample t-test for fast spindles during NREM3 vs. zero: $t(9.68) = 3.57$, $P = 0.005$).

that observed in the control condition (Fig. 6A; relative change in density, mean ± SE: NREM3 = −1.9 ± 0.77%; one sample t-test versus zero: $t(9.02) = -1.07$, $P = 0.31$).

VMA Modulates the Coupling between Fast Spindles and SOs

So far, we have shown a local modulation of adaptation learning on the density of fast spindles during NREM3 but not on the density of SOs. To explore the relevance of the spindle–SO coupling in the consolidation of motor memories, we quantified the amount of spindles locked to a SO during NREM3. Given that only fast spindles were modulated by sleep, we examined the effect of adaptation learning on fast spindle–SO couplings. Even though the proportion of fast spindles coupled with a SO was similar across VMA and CTL sessions (proportion of fast spindles coupled to a SO, mean ± SE: VMA = 31.1 ± 1.1%, CTL = 33.7 ± 1.4%; LMM stats, main effect of session: $F(1, 8.99) = 1.01$, $P = 0.34$), VMA significantly increased the global density of spindle–SO couplings during NREM3 relative to the control (relative change

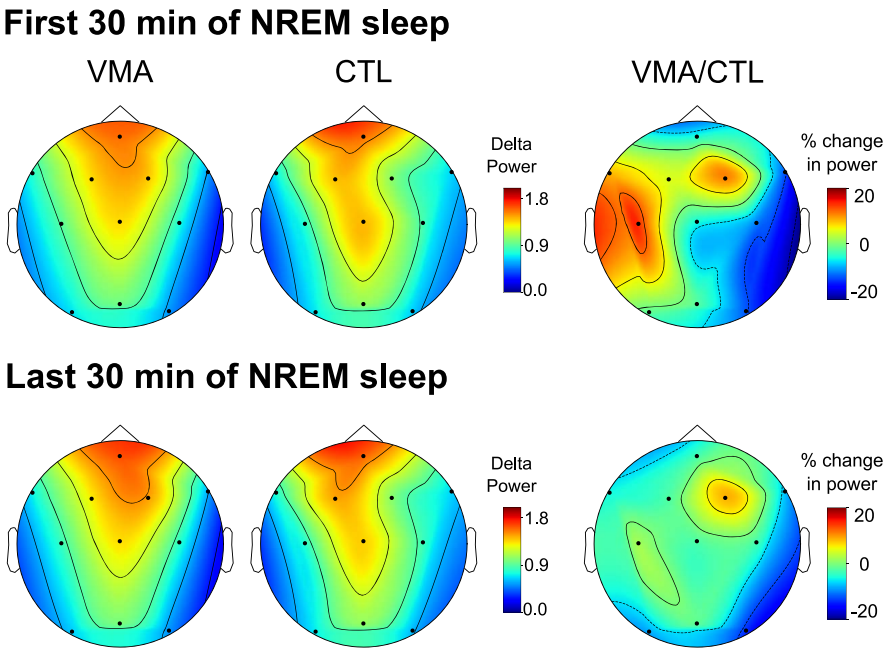

Figure 5. VMA modulates the power of delta activity early during NREM sleep. Shown are the topographic plots for the normalized delta power (1–4 Hz) during the first 30 min (top) and the last 30 min (bottom) of NREM sleep for VMA and CTL sessions and for their relative difference (VMA/CTL). Relative differences were computed according to the function ((VMA − CTL)/CTL*100). Color bars represent the normalized power for the VMA and CTL conditions and the percent change, respectively. As observed for the rest of the metrics quantified in our study, sleep increased the power of delta in an interhemispheric manner, contralateral to the trained hand, during the first versus the last 30 min of NREM sleep ($P = 0.045$).

in density, mean ± SE = 17.48 ± 5.21%; one sample *t*-test versus zero: $t(8.23) = 2.62$, $P = 0.03$). The topographic distribution corresponding to this effect is illustrated in Figure 6*B*.

Further statistical analysis on the relative difference between VMA and CTL yielded a strong interhemispheric modulation, suggesting that this effect was driven by the hemisphere contralateral to the trained hand (relative change in density, mean ± SE: LH: 26.42 ± 9.09%, RH: 1.81 ± 5.88%; LMM stats, main effect of hemisphere: $F(1, 13.8) = 7.03$, $P = 0.019$; followed by a one sample *t*-test for the spindle–SO coupling in the LH versus zero: $t(15.03) = 3.551$, $P = 0.001$).

To examine whether the increment in the fast spindle–SO coupling in fact promoted memory stabilization, we next correlated the relative change in the density of fast spindles associated with a SO during NREM3 with overnight memory retention. To establish further the specificity of this phenomenon, we contrasted this result with that obtained from correlating the relative change in the density of "uncoupled" fast spindles with memory retention. Figure 7 illustrates the correlation for these measures and the corresponding 95% CIs (Fig. 7*A*,*B*) as well as the bootstrapped distribution (Fig. 7*C*,*D*). Only fast spindles associated with a SO predicted overnight memory retention (Pearson correlation: *Coupled fast spindles*: $r1 = 0.73$, CI [0.33 0.95], $P = 0.036$, after adjusting by Bonferroni for two comparisons; *Uncoupled fast spindles*: $r2 = -0.23$, CI [−0.68 0.28], $P = 0.99$, after adjusting by Bonferroni for two comparisons).

In sum, we found that VMA modulates the density of spindles but not their frequency, duration, or amplitude during NREM sleep. This effect was specific for fast spindles during NREM3. Although VMA did not affect the density of SOs, it substantially increased the fast spindle–SO coupling, suggesting that adaptation learning may rather boost the ability of SOs to promote thalamic spindles. Remarkably, adaptation modulated the degree of this coupling locally in an interhermispheric manner, that is, contralateral to the trained hand. The fact that only fast spindles coupled with a SO predicted overnight memory retention points to this association as a potential signature of motor memory consolidation.

Phase Relationship between Sleep Spindles and SOs

Previous studies have shown that learning may influence the degree of synchrony between SOs and spindles, reflected in the level of grouping of spindles around the active phase of the SO (Mölle et al. 2009, 2011). To investigate whether the modulation of the fast spindle–SO coupling observed in Figure 6*B* was associated with a change in the degree of synchrony, we determined the phase of the SO at which the spindle yielded its maximum P-P amplitude and contrasted the level of spindle grouping around the mean phase for the VMA and CTL sessions.

Figure 8 illustrates a consistent phase relationship between SOs and fast spindles for both the CTL and VMA sessions (Rayleigh nonuniformity test. CTL: $r = 0.79$, $P < 0.001$; VMA: $r = 0.96$, $P < 0.001$). In accordance with the declarative literature, fast spindles occurred locked to the active phase of the SO, close to its positive peak (Amzica and Steriade 1998; Steriade and Amzica 1998; Rasch and Born 2013; Ladenbauer et al. 2017; Helfrich et al. 2018; Muehlroth et al. 2019). In addition, we found that the preferred synchronization phase between spindles and SOs (Watson-Williams Test for von Mises Distributions, $F(1, 18) = 2.59$, $P = 0.12$) and the level of grouping around the mean phase (Fisher's test for von Mises Distributions, $F(1, 18) = 0.85$, $P = 0.37$) did not differ across VMA and CTL.

In sum, we showed that fast spindles occurred mainly during the active phase of SOs independently of the condition (CTL or VMA). Even though VMA increased the coupling between

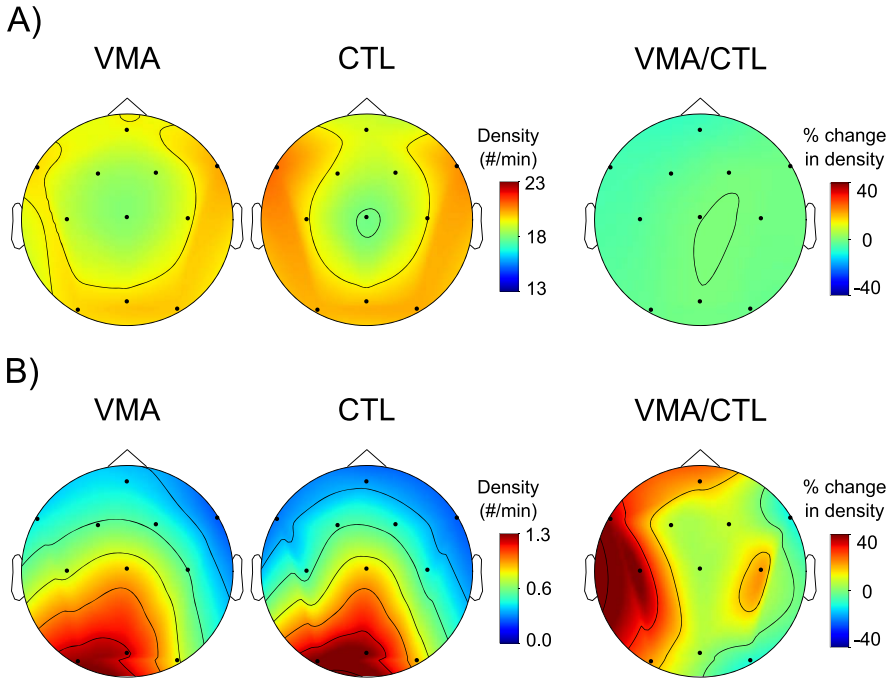

Figure 6. VMA modulates the spindle–SO coupling during NREM3. (*A*) *VMA did not impact on the density of SOs*. Shown are the topographic plots for the density of SOs for the VMA and CTL sessions and their relative difference (VMA/CTL). We found that VMA did not modulate the density of SOs during NREM3 of the first cycle of sleep (one sample *t*-test vs. zero: $t(9.02) = -1.07$, $P = 0.31$). (*B*) *Local modulation of spindle–SO coupling*. Shown are the topographic plots for the density of fast spindles coupled with a SO for the VMA and CTL sessions and their relative difference (VMA/CTL). VMA significantly increased the global density of spindle–SO couplings during NREM3 (one sample *t*-test vs. zero: $t(8.23) = 2.62$, $P = 0.03$). Relative differences were computed according to the function ((VMA − CTL)/CTL*100). Color bars represent the density of these metrics for the VMA and CTL conditions and their percent change, respectively.

SOs and spindles, it did not influence their level of synchrony, suggesting that this parameter may not provide relevant information regarding motor memory stabilization.

Discussion

The degree of coupling between SOs and spindles appears to be critical for sleep-dependent systems consolidation of declarative memories. Here, we examined whether this mechanism operates in the stabilization of motor memories. To this end, we measured the impact of learning a VMA task on the density of SOs, spindles, and their coupling during NREM sleep. Adaptation modulated both the fast spindle density and the degree of fast spindle–SO coupling locally, contralateral to the trained hand during NREM3. Remarkably, the density of fast spindles associated with SOs, but not uncoupled spindles, predicted memory retention overnight, underscoring the importance of this association in the stabilization of procedural memories. Furthermore, adaptation learning increased the power of delta early during NREM sleep, which decreased thereafter, suggesting that VMA may also induce synaptic downscaling locally over the contralateral hemisphere.

The time course of adaptation memory consolidation has remained somewhat elusive for over a decade (Bock et al. 2001; Goedert and Willingham 2002; Caithness et al. 2004; Krakauer et al. 2005; although, see Shadmehr and Brashers-Krug 1997). This likely stems from the failure of retrograde interference protocols at unveiling a gradual recovery of the memory trace in this type of learning (for a comprehensive literature review, refer to Krakauer et al. 2019). Using an alternative anterograde interference approach, we have recently shown evidence supporting the stabilization of VMA memories within a 6-h window post-training (Lerner et al. 2020). This time window is in line with that reported for motor sequence learning (Walker et al. 2003; Korman et al. 2007; Cantarero et al. 2013). Tracking functional connectivity during this period has allowed us to identify a network, including motor, premotor, and posterior parietal areas, mostly contralateral to the trained hand, which peaks at about 6-h post-training and predicts overnight memory retention (Della-Maggiore et al. 2017). Using the same experimental paradigm, here, we identified a sleep-related modulation of brain oscillations over these cortical areas that also predict overnight memory retention. The anatomical congruency is consistent with the hypothesis that sleep promotes the consolidation of memory representations in local networks that may be active during learning (e.g., Klinzing et al. 2019).

There are some major differences worth noticing regarding the neural signatures modulated by learning in our experimental paradigm compared with motor sequence learning. So far, sleep consolidation of motor sequence learning has been linked to changes occurring during NREM2. For example, offline gains in performance correlate positively with the density of sleep spindles (Nishida and Walker 2007; Boutin et al. 2018) as well as with the amount of time spent in NREM2 (Walker et al. 2002; Nishida and Walker 2007). This is in sharp contrast with our study in which VMA modulated the number of spindles exclusively during NREM3. Another important discrepancy between the two types of motor learning is the actual EEG signal affected by training. Overnight improvements in performance associated with motor sequence learning have been linked to an increment

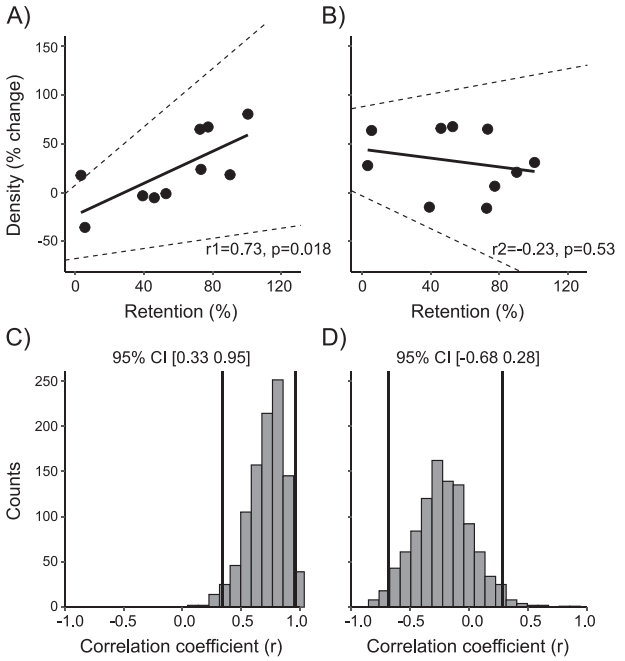

Figure 7. Fast spindles coupled with SOs predict motor memory. *Top panel*. Correlation between the % change ((VMA − CTL)/CTL*100) in the density of fast spindles coupled (*A*) and uncoupled (*B*) with SOs and overnight memory retention. Shown are the dots representing the mean across all four electrodes of the LH for each subject and the corresponding regression lines. Dashed lines depict the limits of the percentile bootstrap 95% CI. *P* values corrected by Bonferroni (alpha/2) are 0.036 and 0.99, respectively. Only fast spindles coupled with SOs predicted overnight memory retention. *Bottom panel*. Distribution of the correlation coefficients between memory retention and the percentage change in the density of coupled (*C*) or uncoupled (*D*) fast spindles, generated after 1000 bootstrap iterations. Vertical black lines indicate the lower and upper limits of the 95% CI.

in the density of uncoupled sleep spindles (Nishida and Walker 2007; Boutin et al. 2018), whereas in our work, only spindles coupled to a SO predicted overnight memory retention. It is important to remark, however, that an enhancement of the coupling between spindles and SOs has also been described in rodents for a type of MSL involving reaching and grasping a pellet through a slit (Silversmith et al. 2020). Further work will be needed to systematically compare motor tasks and establish whether these apparent discrepancies reflect mechanistic differences inherent of the type of learning, the experimental design (e.g., the time elapsed between training and sleep), and/or the sleep stage analyzed (NREM2 vs. NREM3).

Our results show a strong association between the increase in the number of coupled fast spindles and the ability to retain information overnight. The fact that uncoupled spindles were not related to memory retention suggests that only coupled spindles may have promoted memory consolidation. How may the coupling between SOs and fast spindles drive motor memory stabilization? Using two-photon imaging, Niethard and collaborators (2018) found that cortical pyramidal neurons are more sensitive to excitatory inputs during the coupling of these oscillations than during their occurrence alone, which may facilitate dendritic plasticity. It has been proposed that it is during these events that newly encoded representations are reactivated (Steriade et al. 1998). This hypothesis finds support in an MSL study carried out in rodents (Ramanathan et al. 2015), showing task-related neural replay in close temporal association with fast spindles and SOs. We speculate that a similar mechanism based on neural reactivation (Robertson and Genzel 2020) may explain why coupled but not uncoupled spindles predicted overnight memory retention.

The spindle–SO coupling has been proposed as a key association enabling systems consolidation of declarative memories. According to the systems consolidation hypothesis, newly encoded memories, initially stored in hippocampal and cortical networks, are reactivated during slow-wave sleep (SWS) and are gradually integrated with existing memories at the systems level. This process is thought to depend on the close synchrony between SOs, sleep spindles, and hippocampal ripples (Rasch and Born 2007; Diekelmann and Born 2010). Another—not mutually exclusive—account of memory consolidation is the SHY, according to which synaptic weights potentiated during learning are downscaled by sleep (Tononi and Cirelli 2003). By focusing on the renormalization of cortical synapses during SWS, SHY emphasizes the role of sleep in forgetting (Feld and Born 2017), thereby improving the signal-to-noise ratio for strongly potentiated synapses. This process is thought to avoid saturation and benefit memory consolidation. Empirically, SHY would manifest as an increment in the power of delta oscillations during the beginning of sleep that decreases as the night progresses (Tononi and Cirelli 2006; although, see Kuhn et al. 2016 for a theta account of SHY). Our results are in line with both accounts: we found that learning modulated the coupling between fast spindles and SOs as well as the power of delta early during NREM sleep. This opens the possibility that sleep may contribute both to the consolidation of VMA memories as well as the forgetting of irrelevant information.

Finally, it is important to acknowledge that, unlike the work by Tononi and collaborators (Huber et al. 2004; Landsness et al. 2009), a couple of labs have failed to find a beneficial effect of sleep on motor adaptation (Donchin et al. 2002; Doyon et al. 2009; although, refer to Cai and Rickard 2009 for evidence questioning the role of sleep in motor memory consolidation). Yet, we want to emphasize that these studies show substantial methodological differences. For example, Donchin and collaborators used force-field adaptation, an experimental paradigm that differs from VMA in many parameters (such as the level of explicit processing), due to the distinct— proprioceptive —nature of the perturbation (Krakauer et al. 1999; Krakauer et al. 2019). On the other hand, Doyon and collaborators implemented large mirror rotations (180°) that, unlike the small rotation used in our study, are learned and consolidated through different mechanisms (Bédard and Sanes 2011; Gutierrez-Garralda et al. 2013; Telgen et al. 2014). In fact, mirror reversal learning is associated with shifts in time–accuracy tradeoff and offline gains, features that are more common to skill learning tasks than to VMA tasks. Beyond the differences in the experimental paradigms, none of these studies controlled the timing between training and sleep in the way that we and Tononi and collaborators did (practically, 10 min took place between the end of training and bedtime). The close proximity between these events may be key to achieve a stronger benefit of sleep (e.g., Schönauer et al. 2015; Sawangjit et al. 2018).

In conclusion, we have shown that VMA modulates the density of fast spindles and the level of coupling between fast spindles and SOs in a contralateral manner during NREM3. Interestingly, only fast spindles associated with SOs predicted memory retention overnight, pointing to a role of this coupling in motor memory consolidation. In addition, the increase in delta power

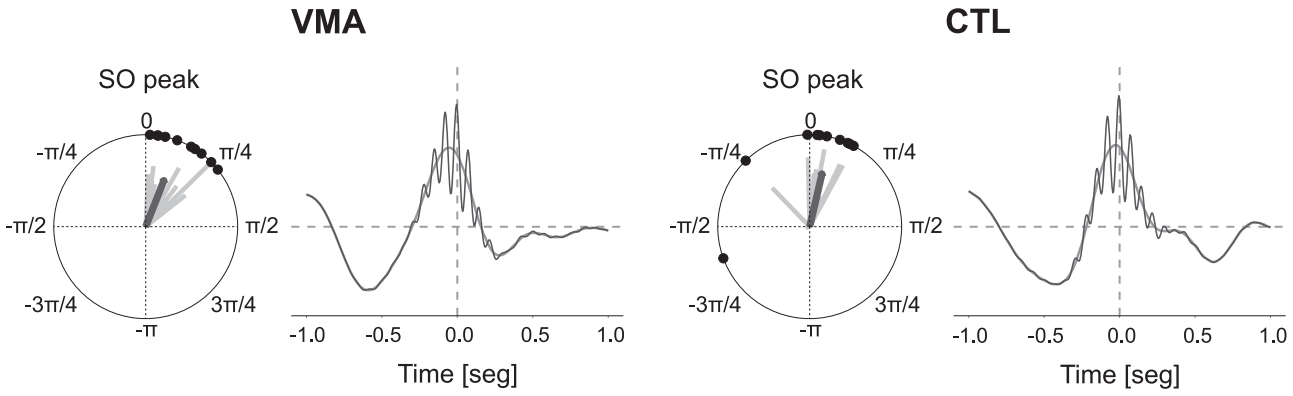

Figure 8. Fast spindle–SO synchrony for VMA and CTL. Shown are the polar plots (left) and the overlaid of fast spindles onto a SO (right) for VMA and CTL. Polar plots illustrate the mean coupling phase between fast spindles and SOs for each subject (gray lines/black dots) and across all subjects (dark gray arrow), corresponding to the LH. Signal overlays depict the grand average of EEG signal for fast spindle–SO coupling events time locked to the spindle's maximum amplitude (time = 0.0), where the gray line is the signal filtered in the SOs frequency band (0.5–1.25 Hz) and the dark gray line is the signal filtered in the fast spindles band (12–16 Hz).

during the initial portion of NREM sleep is consistent with the SHY, suggesting that both these processes may be involved in the stabilization of VMA. Our findings open the possibility of common mechanisms operating at the basis of procedural and declarative memory.

Funding

Argentinian Ministry of Defence (PIDDEF-2014-2017#17); Argentinian Agency for the promotion of Science and Technology (ANPCyT: PICT2015-0844 and PICT2018-1150).

Notes

We thank Juan Belforte for his insightful comments on the manuscript. *Conflict of Interest*: None declared.

References

Agostinelli C, Lund U. 2017. R Package 'Circular': Circular Statistics (Version 0.4-93). https://r-forge.r-project.org/projects/circular/ (last accessed 5 Feb. 2018).

Albouy G, Fogel S, Pottiez H, Nguyen VA, Ray L, Lungu O, Carrier J, Robertson E, Doyon J. 2013. Daytime sleep enhances consolidation of the spatial but not motoric representation of motor sequence memory. *PLoS One*. 8(1):e52805. https://doi.org/10.1371/journal.pone.0052805.

Albouy G, Fogel S, King BR, Laventure S, Benali H, Karni A, Carrier J, Robertson EM, Doyon J. 2015. Maintaining vs. enhancing motor sequence memories: respective roles of striatal and hippocampal systems. *Neuroimage*. 108:423–434. https://doi.org/10.1016/j.neuroimage.2014.12.049.

Albouy G, King BR, Maquet P, Doyon J. 2013. Hippocampus and striatum: dynamics and interaction during acquisition and sleep-related motor sequence memory consolidation. *Hippocampus*. 23(11):985–1004. https://doi.org/10.1002/hipo.22183.

Amzica F, Steriade M. 1998. Electrophysiological correlates of sleep delta waves. *Electroencephalogr Clin Neurophysiol*. 107(2):69–83. https://doi.org/10.1016/s0013-4694(98)00051-0.

Antony JW, Paller KA. 2016. Using oscillating sounds to manipulate sleep spindles. *Sleep*. 40(3):1–8. https://doi.org/10.1093/sleep/zsw068.

Barakat M, Doyon J, Debas K, Vandewalle G, Morin A, Poirier G, Martin N, Lafortune M, Karni A, Ungerleider LG, et al. 2011. Fast and slow spindle involvement in the consolidation of a new motor sequence. *Behav Brain Res*. 217(1):117–121. https://doi.org/10.1016/j.bbr.2010.10.019.

Bates D, Mächler M, Bolker B, Walker S. 2015. Fitting linear mixed-effects models using lme4. *J Stat Softw*. 67(1):1–48. https://doi.org/10.18637/jss.v067.i01.

Bédard P, Sanes JN. 2011. Basal ganglia-dependent processes in recalling learned visual-motor adaptations. *Exp Brain Res*. 209(3):385–393. https://doi.org/10.1007/s00221-011-2561-y.

Bock O, Schneider S, Bloomberg J. 2001. Conditions for interference versus facilitation during sequential sensorimotor adaptation. *Exp Brain Res*. 138:359–365.

Boutin A, Pinsard B, Boré A, Carrier J, Fogel SM, Doyon J. 2018. Transient synchronization of hippocampo-striato-thalamo-cortical networks during sleep spindle oscillations induces motor memory consolidation. *Neuroimage*. 169:419–430. https://doi.org/10.1016/j.neuroimage.2017.12.066.

Brainard DH. 1997. The psychophysics toolbox. *Spat Vis*. 10(4):433–436. https://doi.org/10.1163/156856897x00357.

Buysse DJ, Reynolds CF, Monk TH, Berman SR, Kupfer DJ. 1989. The Pittsburgh sleep quality index: a new instrument for psychiatric practice and research. *Psychiatry Res*. 28(2):193–213. https://doi.org/10.1016/0165-1781(89)90047-4.

Buzsáki G. 2015. Hippocampal sharp wave-ripple: a cognitive biomarker for episodic memory and planning. *Hippocampus*. 25(10):1073–1188. https://doi.org/10.1002/hipo.22488.

Cai DJ, Rickard TC. 2009. Reconsidering the role of sleep for motor memory. *Behav Neurosci*. 123(6):1153.

Caithness G, Osu R, Bays P, Chase H, Klassen J, Kawato M, Wolpert DM, Flanagan JR. 2004. Failure to consolidate the consolidation theory of learning for sensorimotor adaptation tasks. *J Neurosci*. 24:8662–8671.

Cantarero G, Tang B, O'Malley R, Salas R, Celnik P. 2013. Motor learning interference is proportional to occlusion of LTP-like plasticity. *J Neurosci*. 33(11):4634–4641. https://doi.org/10.1523/jneurosci.4706-12.2013.

Cox R, Schapiro AC, Manoach DS, Stickgold R. 2017. Individual differences in frequency and topography of slow and fast sleep spindles. *Front Hum Neurosci*. 11:1–22.

Criscimagna-Hemminger SE, Shadmehr R. 2008. Consolidation patterns of human motor memory. *J Neurosci*.

28(39):9610–9618. https://doi.org/10.1523/jneurosci.3071-08.2008.

DeBruine LM, Barr DJ. 2021. Understanding mixed-effects models through data simulation. *Adv Methods Pract Psychol Sci*. 4(1)1–15. 251524592096511. https://doi.org/10.1177/2515245920965119.

Della-Maggiore V, Villalta JI, Kovacevic N, McIntosh AR. 2017. Functional evidence for memory stabilization in sensorimotor adaptation: a 24-h resting-state fMRI study. *Cereb Cortex*. 27(3):1748–1757. https://doi.org/10.1093/cercor/bhv289.

Delorme A, Makeig S. 2004. EEGLAB: an open source toolbox for analysis of single-trial EEG dynamics including independent component analysis. *J Neurosci Methods*. 134(1):9–21. https://doi.org/10.1016/j.jneumeth.2003.10.009.

Diekelmann S, Born J. 2010. The memory function of sleep. *Nat Rev Neurosci*. 11(2):114–126. https://doi.org/10.1038/nrn2762.

Döhring J, Stoldt A, Witt K, Schönfeld R, Deuschl G, Born J, Bartsch T. 2017. Motor skill learning and offline-changes in TGA patients with acute hippocampal CA1 lesions. *Cortex*. 89:156–168. https://doi.org/10.1016/j.cortex.2016.10.009.

Donchin O, Sawaki L, Madupu G, Cohen LG, Shadmehr R. 2002. Mechanisms influencing acquisition and recall of motor memories. *J Neurophysiol*. 88(4):2114–2123. https://doi.org/10.1152/jn.2002.88.4.2114.

Doyon J, Korman M, Morin A, Dostie V, Tahar AH, Benali H, Karni A, Ungerleider LG, Carrier J. 2009. Contribution of night and day sleep vs. simple passage of time to the consolidation of motor sequence and visuomotor adaptation learning. *Exp Brain Res*. 195(1):15–26. https://doi.org/10.1007/s00221-009-1748-y.

Efron B, Tibshirani R. 1993. *An introduction to the bootstrap*. London: Chapman and Hall/CRC.

Feld GB, Born J. 2017. Sculpting memory during sleep: concurrent consolidation and forgetting. *Curr Opin Neurobiol*. 44:20–27.

Ferrarelli F, Huber R, Peterson MJ, Massimini M, Murphy M, Riedner BA, Watson A, Bria P, Tononi G. 2007. Reduced sleep spindle activity in schizophrenia patients. *Am J Psychiatry*. 164(3):483–492. https://doi.org/10.1176/ajp.2007.164.3.483.

Geva-Sagiv M, Nir Y. 2019. Local sleep oscillations: implications for memory consolidation. *Front Neurosci*. 13:1–7. https://doi.org/10.3389/fnins.2019.00813.

Goedert KM, Willingham DB. 2002. Patterns of interference in sequence learning and prism adaptation inconsistent with the consolidation hypothesis. *Learn Mem*. 9(5):279–292. https://doi.org/10.1101/lm.50102.

Gramfort A, Luessi M, Larson E, Engemann DA, Strohmeier D, Brodbeck C, Goj R, Jas M, Brooks T, Parkkonen L, et al. 2013. MEG and EEG data analysis with MNE-python. *Front Neurosci*. 7:267. https://doi.org/10.3389/fnins.2013.00267.

Gutierrez-Garralda JM, Moreno-Briseño P, Boll MC, Morgado-Valle C, Campos-Romo A, Diaz R, Fernandez-Ruiz J. 2013. The effect of Parkinson's disease and Huntington's disease on human visuomotor learning. *Eur J Neurosci* 38(1):2933–2940. https://doi.org/10.1111/ejn.12288.

Halekoh U, Højsgaard S. 2014. A Kenward-Roger approximation and parametric bootstrap methods for tests in linear mixed models – the R package pbkrtest. *J Stat Softw*. 59(9)1–32. https://doi.org/10.18637/jss.v059.i09.

Helfrich RF, Mander BA, Jagust WJ, Knight RT, Walker MP. 2018. Old brains come uncoupled in sleep: slow wave-spindle synchrony, brain atrophy, and forgetting. *Neuron*. 97(1):221–230.e4. https://doi.org/10.1016/j.neuron.2017.11.020.

Hoddes E, Zarcone V, Smythe H, Phillips R, Dement WC. 1973. Quantification of sleepiness: a new approach. *Psychophysiology*. 10(4):431–436. https://doi.org/10.1111/j.1469-8986.1973.tb00801.x.

Huber R, Felice Ghilardi M, Massimini M, Tononi G. 2004. Local sleep and learning. *Nature*. 430(6995):78–81. https://doi.org/10.1038/nature02663.

Iber C. 2004. Development of a new manual for characterizing sleep. *Sleep*. 27(2):190–192. https://doi.org/10.1093/sleep/27.2.190.

Jacobacci F, Armony JL, Yeffal A, Lerner G, Amaro E, Jovicich J, Doyon J, Della-Maggiore V. 2020. Rapid hippocampal plasticity supports motor sequence learning. *Proc Natl Acad Sci*. 117(38):23898–23903. https://doi.org/10.1073/pnas.2009576117.

Johns MW. 1991. A new method for measuring daytime sleepiness: the Epworth sleepiness scale. *Sleep*. 14(6):540–545. https://doi.org/10.1093/sleep/14.6.540.

Johnson LA, Blakely T, Hermes D, Hakimian S, Ramsey NF, Ojemann JG. 2012. Sleep spindles are locally modulated by training on a brain-computer interface. *Proc Natl Acad Sci*. 109(45):18583–18588. https://doi.org/10.1073/pnas.1207532109.

Kleiner M, Brainard D, Pelli D, Ingling A, Murray R, Broussard C. 2007. What's new in psychtoolbox-3. *Perception*. 36(14):1–16.

Klinzing JG, Niethard N, Born J. 2019. Mechanisms of systems memory consolidation during sleep. *Nat Neurosci*. 22(10):1598–1610. https://doi.org/10.1038/s41593-019-0467-3.

Korman M, Doyon J, Doljansky J, Carrier J, Dagan Y, Karni A. 2007. Daytime sleep condenses the time course of motor memory consolidation. *Nat Neurosci*. 10(9):1206–1213. https://doi.org/10.1038/nn1959.

Krakauer JW, Ghez C, Ghilardi MF. 2005. Adaptation to visuomotor transformations: consolidation, interference and forgetting. *J Neurosci*. 25:473–478.

Krakauer JW, Ghilardi MF, Ghez C. 1999. Independent learning of internal models for kinematic and dynamic control of reaching. *Nat Neurosci*. 2(11):1026–1031. https://doi.org/10.1038/14826.

Krakauer JW, Hadjiosif AM, Xu J, Wong AL, Haith AM. 2019. Motor learning. *Comprehensive physiology*. 9(2):613–663. https://doi.org/10.1002/cphy.c170043.

Kumle L, Võ MLH, Draschkow D. 2021. Estimating power in (generalized) linear mixed models: an open introduction and tutorial in R. *Behav Res Methods*. https://doi.org/10.3758/s13428-021-01546-0.

Kuhn M, Wolf E, Maier JG, Mainberger F, Feige B, Schmid H, Bürklin J, Maywald S, Mall V, Jung NH, et al. 2016. Sleep recalibrates homeostatic and associative synaptic plasticity in the human cortex. *Nat Commun*. 7(1):1–9. https://doi.org/10.1038/ncomms12455.

Ladenbauer J, Ladenbauer J, Külzow N, de Boor R, Avramova E, Grittner U, Flöel A. 2017. Promoting sleep oscillations, their functional coupling by transcranial stimulation enhances memory consolidation in mild cognitive impairment. *J Neurosci*. 37(30):7111–7124. https://doi.org/10.1523/jneurosci.0260-17.2017.

Landsness EC, Crupi D, Hulse BK, Peterson MJ, Huber R, Ansari H, Coen M, Cirelli C, Benca RM, Ghilardi MF, et al. 2009. Sleep-dependent improvement in visuomotor learning: a causal role for slow waves. *Sleep*. 32(10):1273–1284. https://doi.org/10.1093/sleep/32.10.1273.

Latchoumane CFV, Ngo HVV, Born J, Shin HS. 2017. Thalamic spindles promote memory formation during sleep through triple phase-locking of cortical, thalamic, and hippocampal rhythms. *Neuron*. 95(2):424–435.e6. https://doi.org/10.1016/j.neuron.2017.06.025.

Lerner G, Albert S, Caffaro PA, Villalta JI, Jacobacci F, Shadmehr R, Della-Maggiore V. 2020. The origins of anterograde interference in visuomotor adaptation. *Cereb Cortex*. 30(7):4000–4010. https://doi.org/10.1093/cercor/bhaa016.

Leys C, Ley C, Klein O, Bernard P, Licata L. 2013. Detecting outliers: do not use standard deviation around the mean, use absolute deviation around the median. *J Exp Soc Psychol*. 49(4):764–766. https://doi.org/10.1016/j.jesp.2013.03.013.

Maingret N, Girardeau G, Todorova R, Goutierre M, Zugaro M. 2016. Hippocampo-cortical coupling mediates memory consolidation during sleep. *Nat Neurosci*. 19(7):959–964. https://doi.org/10.1038/nn.4304.

Mizrahi-Kliger AD, Kaplan A, Israel Z, Bergman H. 2018. Desynchronization of slow oscillations in the basal ganglia during natural sleep. *Proc Natl Acad Sci*. 115(18):E4274–E4283. https://doi.org/10.1073/pnas.1720795115.

Mölle M, Bergmann TO, Marshall L, Born J. 2011. Fast and slow spindles during the sleep slow oscillation: disparate coalescence and engagement in memory processing. *Sleep*. 34(10):1411–1421. https://doi.org/10.5665/sleep.1290.

Mölle M, Eschenko O, Gais S, Sara SJ, Born J. 2009. The influence of learning on sleep slow oscillations and associated spindles and ripples in humans and rats. *Eur J Neurosci*. 29(5):1071–1081. https://doi.org/10.1111/j.1460-9568.2009.06654.x.

Morin A, Doyon J, Dostie V, Barakat M, Tahar AH, Korman M, Benali H, Karni A, Ungerleider LG, Carrier J. 2008. Motor sequence learning increases sleep spindles and fast frequencies in post-training sleep. *Sleep*. 31(8):1149–1156. https://doi.org/10.5665/sleep/31.8.1149.

Muehlroth BE, Sander MC, Fandakova Y, Grandy TH, Rasch B, Shing YL, Werkle-Bergner M. 2019. Precise slow oscillation–spindle coupling promotes memory consolidation in younger and older adults. *Sci Rep*. 9(1):1940. https://doi.org/10.1038/s41598-018-36557-z.

Mullen TR, Kothe CAE, Chi YM, Ojeda A, Kerth T, Makeig S, Jung TP, Cauwenberghs G. 2015. Real-time neuroimaging and cognitive monitoring using wearable dry EEG. *IEEE Trans Biomed Eng*. 62(11):2553–2567. https://doi.org/10.1109/tbme.2015.2481482.

Navarro-Lobato I, Genzel L. 2019. The up and down of sleep: from molecules to electrophysiology. *Neurobiol Learn Mem*. 160:3–10. https://doi.org/10.1016/j.nlm.2018.03.013.

Niethard N, Ngo HVV, Ehrlich I, Born J. 2018. Cortical circuit activity underlying sleep slow oscillations and spindles. *Proc Natl Acad Sci*. 115(39):E9220–E9229. https://doi.org/10.1073/pnas.1805517115.

Niknazar M, Krishnan GP, Bazhenov M, Mednick SC. 2015. Coupling of thalamocortical sleep oscillations are important for memory consolidation in humans. *PLoS One*. 10(12):e0144720. https://doi.org/10.1371/journal.pone.0144720.

Nishida M, Walker MP. 2007. Daytime naps, motor memory consolidation and regionally specific sleep spindles. *PLoS One*. 2(4):e341. https://doi.org/10.1371/journal.pone.0000341.

Oldfield RC. 1971. The assessment and analysis of handedness: the Edinburgh inventory. *Neuropsychologia*. 9(1):97–113. https://doi.org/10.1016/0028-3932(71)90067-4.

Oostenveld R, Praamstra P. 2001. The five percent electrode system for high-resolution EEG and ERP measurements. *Clin Neurophysiol*. 112(4):713–719. https://doi.org/10.1016/s1388-2457(00)00527-7.

Pewsey A, Neuhäuser M, Ruxton GD. 2013. *Circular statistics in R*. Oxford(UK): Oxford University Press.

Plihal W, Born J. 1997. Effects of early and late nocturnal sleep on declarative and procedural memory. *J Cogn Neurosci*. 9(4):534–547. https://doi.org/10.1162/jocn.1997.9.4.534.

R Core Team. 2017. *R: a language and environment for statistical computing*. Vienna, Austria: R Foundation for Statistical Computing, https://www.R-project.org/.

Ramanathan DS, Gulati T, Ganguly K. 2015. Sleep-dependent reactivation of ensembles in motor cortex promotes skill consolidation. *PLoS Biol*. 13(9):e1002263. https://doi.org/10.1371/journal.pbio.1002263.

Rasch B, Born J. 2007. Maintaining memories by reactivation. *Curr Opin Neurobiol*. 17(6):698–703. https://doi.org/10.1016/j.conb.2007.11.007.

Rasch B, Born J. 2013. About sleep's role in memory. *Physiol Rev*. 93(2):681–766. https://doi.org/10.1152/physrev.00032.2012.

Rasch B, Buchel C, Gais S, Born J. 2007. Odor cues during slow-wave sleep prompt declarative memory consolidation. *Science*. 315(5817):1426–1429. https://doi.org/10.1126/science.1138581.

Riedner BA, Vyazovskiy VV, Huber R, Massimini M, Esser S, Murphy M, Tononi G. 2007. Sleep homeostasis and cortical synchronization: III. A high-density EEG study of sleep slow waves in humans. *Sleep*. 30(12):1643–1657. https://doi.org/10.1093/sleep/30.12.1643.

Robertson EM, Genzel L. 2020. Memories replayed: reactivating past successes and new dilemmas. *Philos Trans R Soc B Biol Sci*. 375(1799):20190226. https://doi.org/10.1098/rstb.2019.0226.

RStudio Team. 2015. *RStudio: integrated development for R*. Boston (MA): RStudio, Inc, http://www.rstudio.com/.

Sawangjit A, Oyanedel CN, Niethard N, Salazar C, Born J, Inostroza M. 2018. The hippocampus is crucial for forming non-hippocampal long-term memory during sleep. *Nature*. 564(7734):109–113. https://doi.org/10.1038/s41586-018-0716-8.

Schapiro AC, Reid AG, Morgan A, Manoach DS, Verfaellie M, Stickgold R. 2019. The hippocampus is necessary for the consolidation of a task that does not require the hippocampus for initial learning. *Hippocampus*. 29(11):1091–1100. https://doi.org/10.1002/hipo.23101.

Schönauer M, Pöhlchen D. 2018. Sleep spindles. *Curr Biol*. 28(19):R1129–R1130. https://doi.org/10.1016/j.cub.2018.07.035.

Schönauer M, Grätsch M, Gais S. 2015. Evidence for two distinct sleep-related long-term memory consolidation processes. *Cortex*. 63:68–78. https://doi.org/10.1016/j.cortex.2014.08.005.

Shadmehr R, Brashers-Krug T. 1997. Functional stages in the formation of human long-term motor memory. *J Neurosci*. 17(1):409–419.

Silversmith DB, Lemke SM, Egert D, Berke JD, Ganguly K. 2020. The degree of nesting between spindles and slow oscillations modulates neural synchrony. *J Neurosci*. 40(24):4673–4684. https://doi.org/10.1523/jneurosci.2682-19.2020.

Staresina BP, Bergmann TO, Bonnefond M, van der Meij R, Jensen O, Deuker L, Elger CE, Axmacher N, Fell J. 2015. Hierarchical nesting of slow oscillations, spindles and ripples in the human hippocampus during sleep. *Nat Neurosci*. 18(11):1679–1686. https://doi.org/10.1038/nn.4119.

Steriade M. 2006. Grouping of brain rhythms in corticothalamic systems. *Neuroscience*. 137(4):1087–1106. https://doi.org/10.1016/j.neuroscience.2005.10.029.

Steriade M, Amzica F. 1998. Coalescence of sleep rhythms and their chronology in corticothalamic networks. *Sleep Res Online*. 1(1):1–10 ISSN: 1096-214X.

Steriade M, Timofeev I, Grenier F, Dürmüller N. 1998. Role of thalamic and cortical neurons in augmenting responses and self-sustained activity: dual intracellular recordings in vivo. *J Neurosci*. 18(16):6425–6443. https://doi.org/10.1523/jneurosci.18-16-06425.1998.

Tamaki M, Bang JW, Watanabe T, Sasaki Y. 2016. Night watch in one brain hemisphere during sleep associated with the first-night effect in humans. *Curr Biol*. 26(9):1190–1194. https://doi.org/10.1016/j.cub.2016.02.063.

Telgen S, Parvin D, Diedrichsen J. 2014. Mirror reversal and visual rotation are learned and consolidated via separate mechanisms: Recalibrating or learning de novo? *J Neurosci*. 34(41):13768–13779. https://doi.org/10.1523/jneurosci.5306-13.2014.

Timofeev I, Grenier F, Bazhenov M, Sejnowski TJ, Steriade M. 2000. Origin of slow cortical oscillations in deafferented cortical slabs. *Cereb Cortex*. 10(12):1185–1199. https://doi.org/10.1093/cercor/10.12.1185.

Tononi G, Cirelli C. 2003. Sleep and synaptic homeostasis: a hypothesis. *Brain Res Bull*. 62(2):143–150. https://doi.org/10.1016/j.brainresbull.2003.09.004.

Tononi G, Cirelli C. 2006. Sleep function and synaptic homeostasis. *Sleep Med Rev*. 10(1):49–62. https://doi.org/10.1016/j.smrv.2005.05.002.

Tort ABL, Komorowski R, Eichenbaum H, Kopell N. 2010. Measuring phase-amplitude coupling between neuronal oscillations of different frequencies. *J Neurophysiol*. 104(2):1195–1210. https://doi.org/10.1152/jn.00106.2010.

Villalta JI, Landi SM, Flo A, Della-Maggiore V. 2015. Extinction interferes with the retrieval of visuomotor memories through a mechanism involving the sensorimotor cortex. *Cereb Cortex*. 25(6):1535–1543. https://doi.org/10.1093/cercor/bht346.

Walker MP, Brakefield T, Allan Hobson J, Stickgold R. 2003. Dissociable stages of human memory consolidation and reconsolidation. *Nature*. 425(6958):616–620. https://doi.org/10.1038/nature01930.

Walker MP, Brakefield T, Morgan A, Hobson JA, Stickgold R. 2002. Practice with sleep makes perfect. *Neuron*. 35(1):205–211. https://doi.org/10.1016/s0896-6273(02)00746-8.

Wamsley EJ. 2019. Memory consolidation during waking rest. *Trends Cogn Sci*. 23(3):171–173.

Wang SY, Baker KC, Culbreth JL, Tracy O, Arora M, Liu T, Morris S, Collins MB, Wamsley EJ. 2021. 'Sleep-dependent' memory consolidation? Brief periods of post-training rest and sleep provide an equivalent benefit for both declarative and procedural memory. *Learn Mem*. 28(6):195–203. https://doi.org/10.1101/lm.053330.120.

Wilhelm I, Kurth S, Ringli M, Mouthon AL, Buchmann A, Geiger A, Jenni OG, Huber R. 2014. Sleep slow-wave activity reveals developmental changes in experience-dependent plasticity. *J Neurosci*. 34(37):12568–12575. https://doi.org/10.1523/jneurosci.0962-14.2014.